Development of Naphthalene PLIF for Visualizing Ablation Products from a Space Capsule Heat Shield

C. S. Combs[1], N. T. Clemens[2]
The University of Texas, Austin TX, 78712

and

P. M. Danehy[3]
NASA Langley Research Center, Hampton, VA, 23681-2199

The Orion Multi-Purpose Crew Vehicle (MPCV) will use an ablative heat shield. To better design this heat shield and others that will undergo planetary entry, an improved understanding of the ablation process would be beneficial. Here, a technique developed at The University of Texas at Austin that uses planar laser-induced fluorescence (PLIF) of a low-temperature sublimating ablator (naphthalene) to enable visualization of the ablation products in a hypersonic flow is applied. Although high-temperature ablation is difficult and expensive to recreate in a laboratory environment, low-temperature sublimation creates a limited physics problem that can be used to explore ablation-product transport in a hypersonic flow-field. In the current work, a subscale capsule reentry vehicle model with a solid naphthalene heat shield has been tested in a Mach 5 wind tunnel. The PLIF technique provides images of the spatial distribution of sublimated naphthalene in the heat-shield boundary layer, separated shear layer, and backshell recirculation region. Visualizations of the capsule shear layer using both naphthalene PLIF and Schlieren imaging compared favorably. PLIF images have shown high concentrations of naphthalene in the capsule separated flow region, intermittent turbulent structures on the heat shield surface, and interesting details of the capsule shear layer structure. It was shown that, in general, the capsule shear layer appears to be more unsteady at lower angels of attack. The PLIF images demonstrated that during a wind tunnel run, as the model heated up, the rate of naphthalene ablation increased, since the PLIF signal increased steadily over the course of a run. Additionally, the shear layer became increasingly unsteady over the course of a wind tunnel run, likely because of increased surface roughness but also possibly because of the increased blowing. Regions with a relatively low concentration of naphthalene were also identified in the capsule backshell recirculation region and are most likely the result of cross-flow-induced vortices on the capsule afterbody.

Nomenclature

AoA	=	Angle-of-Attack
CFD	=	Computational Fluid Dynamics
CO_2	=	Carbon Dioxide
FWHM	=	Full-Width at Half Maximum
LES	=	Large-Eddy Simulations
MPCV	=	Multi-Purpose Crew Vehicle
MSDS	=	Material Safety Data Sheet
NO	=	Nitric Oxide
OH	=	Hydroxyl Radical
PAH	=	Polycyclic Aromatic Hydrocarbon

[1] Graduate Student, Department of Aerospace Engineering & Engineering Mechanics, Member AIAA.
[2] Bob R. Dorsey Professor in Engineering, Department of Aerospace Engineering & Engineering Mechanics, Associate Fellow AIAA.
[3] Research Scientist, Advanced Sensing and Optical Measurement Branch, MS 493, Associate Fellow AIAA.

PLIF = Planar Laser-Induced Fluorescence
RANS = Reynolds-Averaged Navier Stokes Equations
Re_D = Reynolds Number based on Model Diameter
TPS = Thermal Protection System
UV = Ultra-violet
ViDI = Virtual Diagnostics Interface

I. Introduction

NASA has continued interest in the study of ablation owing to the need to develop suitable thermal protection systems (TPS) for spacecraft that undergo planetary entry. Ablation is a complex multi-physics process, and codes that predict it require a number of coupled submodels, each of which requires validation.[1] For example, Reynolds-averaged Navier Stokes (RANS) and large-eddy simulation (LES) codes require models of the turbulent transport of ablation products under variable compressibility and pressure gradient conditions; however, suitable scalar-velocity data under relevant conditions are very rare.[2] A new technique has been developed at The University of Texas at Austin that uses planar laser-induced fluorescence (PLIF) of a low-temperature sublimating ablator (naphthalene) to enable visualization of the ablation products in a hypersonic flow.[3] While high temperature ablation is difficult and expensive to recreate in a laboratory environment and while high-temperature ablation is a very complex process involving nonequilibrium gaseous and surface chemistry, spallation, radiation, etc., low temperature ablation creates a limited physics problem that can be used to simulate the ablation process. Naphthalene,[4] camphor,[5] wax,[6] CO_2 (dry ice),[7] and water-ice[8]—all low-temperature sublimating ablators—have been used previously to study ablation, with camphor and CO_2 being employed most often. Determining ablation rates of cones, hemispheres, and other projectile-like models has been the focus of the majority of ablation studies performed using low-temperature sublimating ablators.[9]

Experiments taking advantage of naphthalene sublimation have also been used to study boundary layer transition, heat transfer, and mass transfer.[10,11] These techniques generally employ a thin film of naphthalene coated onto the surface of the model. The model can simply be weighed before and after a test or the recession of the naphthalene layer can be measured in order to perform a mass transfer experiment. Using a heat/mass transfer analogy, heat transfer rates can be inferred from these results. When studying turbulent transition, the thin film of naphthalene will rapidly sublimate off the model surface in regions where the boundary layer is turbulent, allowing one to determine the location of transition by visually inspecting the model.[12]

PLIF is a well-developed non-intrusive flow diagnostic technique that provides a qualitative two-dimensional visualization of scalar concentration in a flow.[13] PLIF uses a laser sheet to interrogate a slice in the flow containing the species of interest, which in this case is naphthalene vapor. This ultraviolet (UV) laser sheet excites the naphthalene molecules, resulting in fluorescence that is detected by a digital camera. When factors affecting the fluorescence intensity such as collisional quenching, temperature, and optical collection efficiencies are considered, the PLIF signal can sometimes be converted into species number density and/or mole fraction. Numerous flow fields have been studied using PLIF of species such as acetone,[14] NO, [15] and OH.[16] PLIF has also been used to investigate various capsule geometries in high speed flows.[17-20] Naphthalene PLIF was originally introduced as a fuel-marking technique in low-speed reacting flow experiments[21] but only recently has the technique been used to image ablation products in a supersonic turbulent boundary layer.[3]

NASA researchers have used NO PLIF to simulate the ablation process by transpiring NO gas through a port on the surface of a capsule model.[22] However, the advantage of using a low-temperature sublimating ablator is that the transported products are the result of mass transfer from the heat shield itself. In the current work a subscale capsule reentry vehicle model with a solid naphthalene heat shield has been tested in a Mach 5 wind tunnel. This technique enables the distribution of the ablation products as they are transported into the boundary layer and over the capsule shoulder to be revealed by PLIF imaging. These images can help provide insight into scalar transport, flow structure, and potentially provide validation data for scalar-transport models.

II. Experimental Program

A. Experimental Facility

The facility used for these experiments was a Mach 5 blow-down wind tunnel. The cross-section of the test section of the facility was 152 mm wide by 178 mm tall. Optical access for laser transmission and imaging was provided by fused silica windows on the wind tunnel floor, ceiling, and sidewall. The wind tunnel was supplied by a 4 m^3 storage tank held at approximately 15.5 MPa and the plenum pressure was maintained at approximately 2.48 MPa. The flow was electrically heated to achieve a stagnation temperature of about 360 K in order to increase the

sublimation rate of the naphthalene heat shield. These conditions resulted in a Reynolds number based on model diameter (Re_D) of 10^6.

B. Naphthalene Chemistry

Naphthalene, $C_{10}H_8$, is a polycyclic aromatic hydrocarbon (PAH) and is a byproduct of many combustion processes. Crystalline/powder-form 99% naphthalene was purchased from Acros Organics for use in this study. A white crystalline solid at room temperature, naphthalene has a relatively low melting point at 353 K. The low melting point allows naphthalene crystals to easily be melted down and used for making molds of various shapes and sizes. The vapor pressure of naphthalene is approximately 12 Pa at 300 K, but increases by over two orders of magnitude to 1.4 kPa at 360 K.[23] When working with naphthalene, naphthalene vapor will always be present in the laboratory environment, and the material safety data sheet (MSDS) for naphthalene recommends wearing gloves, goggles, a dust respirator, and a lab coat. Although naphthalene is stable (given a zero out of four on the reactivity criterion) it is flammable and can ignite when moderately heated.

A relatively large molecule, naphthalene possesses a wide and essentially continuous band of vibronic energy levels in the UV. Naphthalene absorbs electromagnetic radiation from the vacuum UV to approximately 310 nm.[24] Excitation of naphthalene with a UV light source results in broadband fluorescence between 300 and 400 nm.[24] This property of naphthalene makes it a candidate for PLIF imaging, as high-intensity light sources such as frequency-quadrupled Nd:YAG lasers, KrF lasers, and various dye laser configurations can be used to excite the molecule.

C. Model Geometry

The model geometry for this study consisted of a scaled Orion Multi-Purpose Crew Vehicle (MPCV) shaped model with smooth outer mold lines. The model consisted of an aluminum capsule backshell, a separate heat shield piece, and a wire "mesh" to give the solid naphthalene heat shield structural integrity (Figure 1a). The mesh was mounted to sixteen 6-32 screws that protruded approximately 4 mm from the aluminum surface. The heads of the screws were at least 2 mm below the surface of the heat shield. Thin-gauge wire was then wrapped around the bolts, creating a mesh. Without this mesh, the naphthalene heat shield would not adhere to the aluminum model and would not remain attached during wind tunnel runs. However, even with the mesh, naphthalene would still break apart from the model during wind tunnel startup for some tests. Data from these wind tunnel runs is not presented here, but for this technique to be successful it is important to have a relatively quick wind tunnel startup or to place a protective covering on the model until the freestream flow has been fully established. The aluminum model was scaled to have a 50 mm maximum heat shield diameter and was attached to a 12.7 mm diameter stainless steel sting. The sting was mounted to a strut that was fixed to the wind tunnel floor. Four different strut configurations were used in this experimental campaign, allowing four different angles of attack (0°, 12°, 24°, and 52°) to be tested. Schlieren imaging was conducted in a different experimental campaign than the PLIF and used a solid aluminum heat shield rather than a naphthalene one.

The process for creating the naphthalene heat shield involved placing the capsule model in a mold and pouring heated liquid naphthalene through a hole in the aftbody or "top" of the model. The cylindrical aluminum mold had two parts, shown in Figure 1b. The bottom portion was a 200 mm diameter, 50 mm tall cylinder with a hemispherical bowl having dimensions of a scaled heat shield geometry machined into its top surface and eight tapped bolt holes in a circular pattern for securing the two halves of the mold. It was imperative that the mold be extremely smooth prior to pouring. Over time, scratches and chips accumulated on the surface of the mold, leading to naphthalene sticking to the mold rather than the model. For this reason, the mold would occasionally be polished to remove any imperfections. The top portion of the mold was a 200 mm diameter, 25 mm tall cylinder with a centered cutout contoured to fit the backshell model and eight thru-holes for bolts. To prepare the mold, the model was rested on top of the bottom half of the mold. The top half of the mold was then placed over the model and the two halves of the mold were secured with bolts. The complete mold assembly can be seen in Figure 1c. This assembly allowed the aft portion of the MPCV model to protrude from the top of the mold, exposing the hole drilled through the center of the aluminum model to be used for pouring liquid naphthalene into the mold. Wearing proper protective equipment, approximately 150 mL of naphthalene crystals was then placed in a beaker under a fume hood. This beaker would then be heated on a hot plate until the naphthalene had been completed melted. A funnel was then placed in the hole for pouring liquid naphthalene, and the naphthalene was poured into the mold. To ensure that the mold was full, naphthalene was poured until the liquid was overflowing out of the top of the mold. The mold assembly would then be allowed to cool at room temperature for approximately three hours to allow the naphthalene to solidify. Next, the mold would be disassembled and any excess naphthalene on the capsule backshell would be carefully removed to ensure that the naphthalene-aluminum junction was smooth. It was also verified that no air

pockets were formed in the naphthalene during the molding process. At this point the model was ready for testing and was mounted in the Mach 5 wind tunnel test section. During wind tunnel shutdown, the remaining naphthalene on the model was destroyed, preventing images of the model from being captured post-run. A new heat shield was molded before each wind tunnel run and a completed model is shown in Figure 2 below.

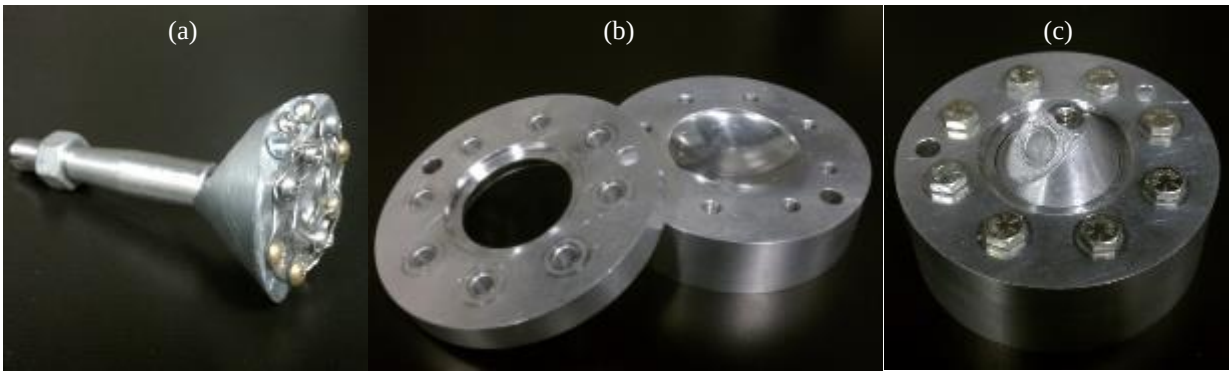

Figure 1: (a) Orion MPCV model and sting without naphthalene heat shield, (b) top and bottom halves of mold assembly for creating naphthalene heat shield, and (c) fully-assembled mold with capsule model installed, ready for liquid naphthalene.

Figure 2: Orion MPCV model at 52° angle of attack configuration with naphthalene heat shield installed in the Mach 5 wind tunnel facility at The University of Texas at Austin.

D. Experimental Setup

PLIF of naphthalene vapor was used to obtain a qualitative measure of the concentration of ablation products in the flow. The laser system consisted of a frequency-quadrupled Nd:YAG laser with a 266 nm output operating at a rate of 10 Hz. This wavelength was selected to excite naphthalene vapor molecules, which absorb UV radiation as discussed earlier. The laser energy was maintained at approximately 30 mJ/pulse, corresponding to an irradiance of 18 kW/mm^2, in order to remain below the saturation threshold of the naphthalene vapor, based on previous research.[3] It was also confirmed that the ablation process was not significantly altered by the laser impinging on the surface of the model. The UV laser beam was oriented by a series of laser mirrors so that it passed up to the top of the wind tunnel facility where it was formed into a laser sheet using conventional sheet forming optics, as seen in Figure 3. The resulting laser sheet was about 1 mm thick (FWHM) in the measurement region and approximately 75 mm wide. The naphthalene fluorescence was imaged onto a back-illuminated CCD camera (Apogee Alta U47), which had quantum efficiency of about 57% in the near UV and read noise of 9 e^- RMS. The camera was oriented normal to the laser sheet. The camera was fitted with a 100 mm focal length f/2.8 UV lens (Cerco) operated at full aperture and included a 20 mm extension ring for close focusing. A series of Schott colored glass filters (two WG-295 filters and one UG-11 filter) were placed in front of the lens to block scattered laser light and reduce the amount

of solid state naphthalene fluorescence imaged by the CCD. The imaging field of view was about 50 mm x 50 mm. The images were obtained at a rate of approximately 1/3 Hz with a 30 millisecond exposure time. About 20 images were acquired per wind tunnel run. The experiment was synchronized using several Stanford Research Systems digital delay generators to ensure that images were acquired while the laser was firing.

E. PLIF Flow Visualization Image Processing

Single-shot PLIF images were processed by first removing the background and then were corrected for variations in the mean intensity profile of the laser sheet. Single-shot sheet corrections were not made. The mean laser sheet spatial intensity variation was measured by imaging the fluorescence from a cell filled with acetone vapor. Approximately 20 mL of acetone was placed inside the cell and the cell was immediately closed. The liquid acetone would quickly evaporate, filling the cell with an essentially uniform distribution of acetone vapor. The cell was then placed inside the wind tunnel test section with the capsule model removed, allowing the acetone vapor to be excited with the 266 nm output from the frequency-quadrupled Nd:YAG laser. The fluorescence from the excited acetone vapor molecules was then captured with the same CCD camera used for the PLIF experiments. Since the acetone vapor was distributed uniformly in the cell, the images of the acetone fluorescence provided a two-dimensional laser sheet intensity profile. In order to determine a mean laser-sheet intensity profile, 50 acetone fluorescence images were averaged. The single-shot images obtained during the runs were then divided by this laser-sheet intensity profile to correct for spatial variations in laser energy. No correction was made for potential laser absorption by naphthalene vapor. Additionally, in many of the subsequent figures, the PLIF intensity is presented in a logarithmic scale to improve the visibility of the entire flowfield without saturating other parts of the image.

F. Virtual Diagnostics Interface (ViDI)

The Virtual Diagnostics Interface (ViDI)[25] is a software tool developed at NASA Langley Research Center that provides unified data handling and interactive three-dimensional display of experimental data and computational predictions. It is a combination of custom-developed software applications and Autodesk® 3ds Max®, a commercially available, CAD-like software package for three-dimensional rendering and animation.[26] ViDI technology can be applied to three main areas: 1) pre-test planning and optimization; 2) visualization and analysis of experimental data and/or computational predictions; and 3) establishment of a central hub to visualize, store, and retrieve experimental results. For this experiment, ViDI was used primarily for post-test visualization of the PLIF data as in Reference 27.

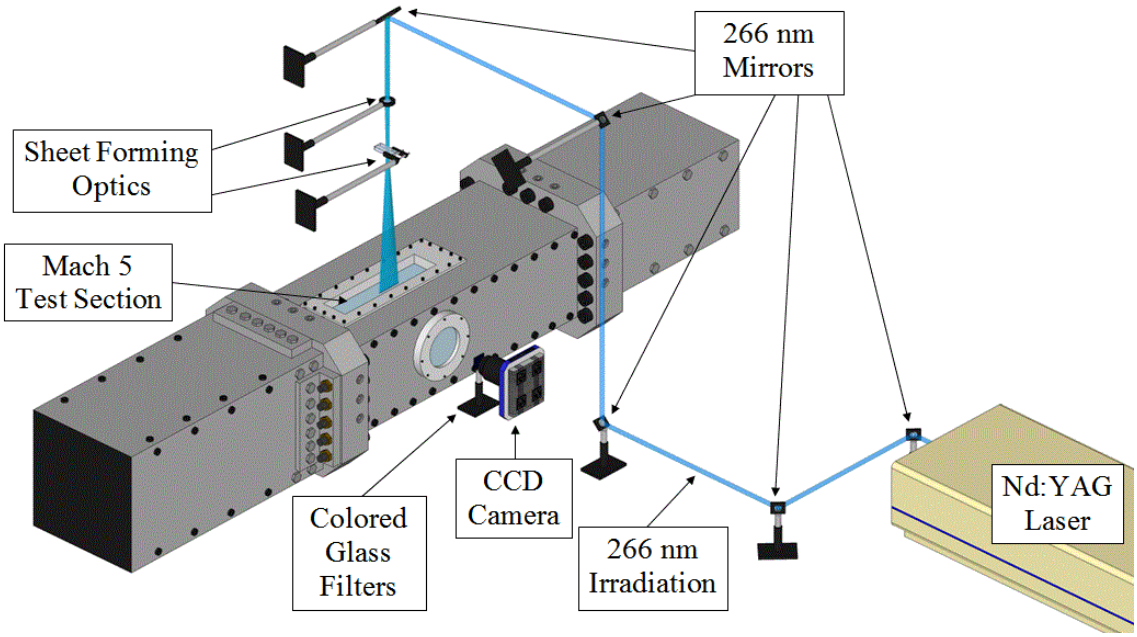

Figure 3: Schematic of the setup used for naphthalene PLIF experiments in the Mach 5 wind tunnel facility. Flow is from bottom left to top right.

III. Experimental Results and Discussion

Naphthalene PLIF images were collected in the Mach 5 wind tunnel facility at The University of Texas at Austin's Pickle Research Campus. Some of these images can be seen in Figures 4 through 7, with each figure representing a time-sequence of PLIF images for a different angle of attack. The elapsed time between image (a) and (f) in each case is approximately one minute. At each angle of attack (Figures 4 through 7), the shear layer is clearly seen since naphthalene accumulates in the afterbody recirculation region. Furthermore, few naphthalene structures are visualized in the heat shield boundary layer, except for the highest angle of attack (Figure 7), which consistently shows turbulent structures near the heat shield surface. This 52° angle of attack case has the longest development length for the boundary layer (from the stagnation point) and it seems to be the most turbulent and the thickest at the leeward shoulder (and hence the easiest to visualize). The 12° case produced intermittent turbulent structures on the heat shield surface. Turbulent structures were not clearly visualized on the heat shield surface for the 0° and 24° case. Considering the 0° case, this is most likely due to the relatively short development length for the boundary layer on the heat shield surface. However, for the 24° case this may be a result of the images in Figure 6 having a lower signal-to-noise ratio than the images in Figures 4 and 5.

The shear layer appears to be laminar in the 24° case, whereas in the 12° and 0° cases the shear layer appears to transition from laminar to turbulent (or at least unsteady) over the course of the run. Not enough naphthalene vapor was visualized in the shear layer for the 52° case to make a determination as to the nature of the shear layer, although the limited evidence suggests a laminar flow. In general, though, the shear layer appeared to be more unsteady at lower angles of attack. Another effect of run time evident in the figures is that the model heats up over the course of the run, leading to more ablation and significantly more naphthalene present in the separated flow region (for each run and corresponding figure, the image intensity was plotted on the same absolute scale).

Additionally, notice in Figures 4-6 that there appears to be a region of relatively low naphthalene signal located near the sting on the capsule afterbody in the wake region. This feature is particularly prominent in Figure 6d, but can be seen in the other images as well. This low-signal region appears to stay in approximately the same location for all the images in Figure 6. In Figures 4 and 5 there is another low-signal region located farther upstream than the one in Figure 6 that also remains in approximately the same position throughout the run. These features are most likely the result of cross-flow induced vortices since they only appear in the cases at higher angles of attack. Another feature, seen most clearly in Figure 5d-f is a series of elongated naphthalene structures that emanate from the upper edge of the shear layer. These structures are nearly vertical in the images, but are at an angle of about 45° with respect to the flow direction. The source of these structures is not known at this time, but it is possible they are turbulent-structures that originate in the upstream boundary layer and then are strained and stretched by the rapid expansion around the leeward shoulder. Another observation, seen in Figures 4 through 6, is that the shear layer appears laminar or transitional at the beginning of the run but may be fully turbulent towards the end of the run (subfigures e and f). Considering that the freestream Reynolds number is effectively constant over the course of the run, the onset of transition is most likely due to the change in the nature of the heat shield surface as a result of the ablation process. As the heat shield ablates, its surface becomes rough, which could lead to transition to turbulence. Additionally, the mass transfer rate or blowing rate of naphthalene vapor on the heat shield surface increases over the course of the run, which could affect turbulent transition. Lastly, the shear layer appears to be most steady near the capsule's leeward shoulder and increasingly unsteady further downstream, which is consistent with previous investigations of capsule shear layers.[20]

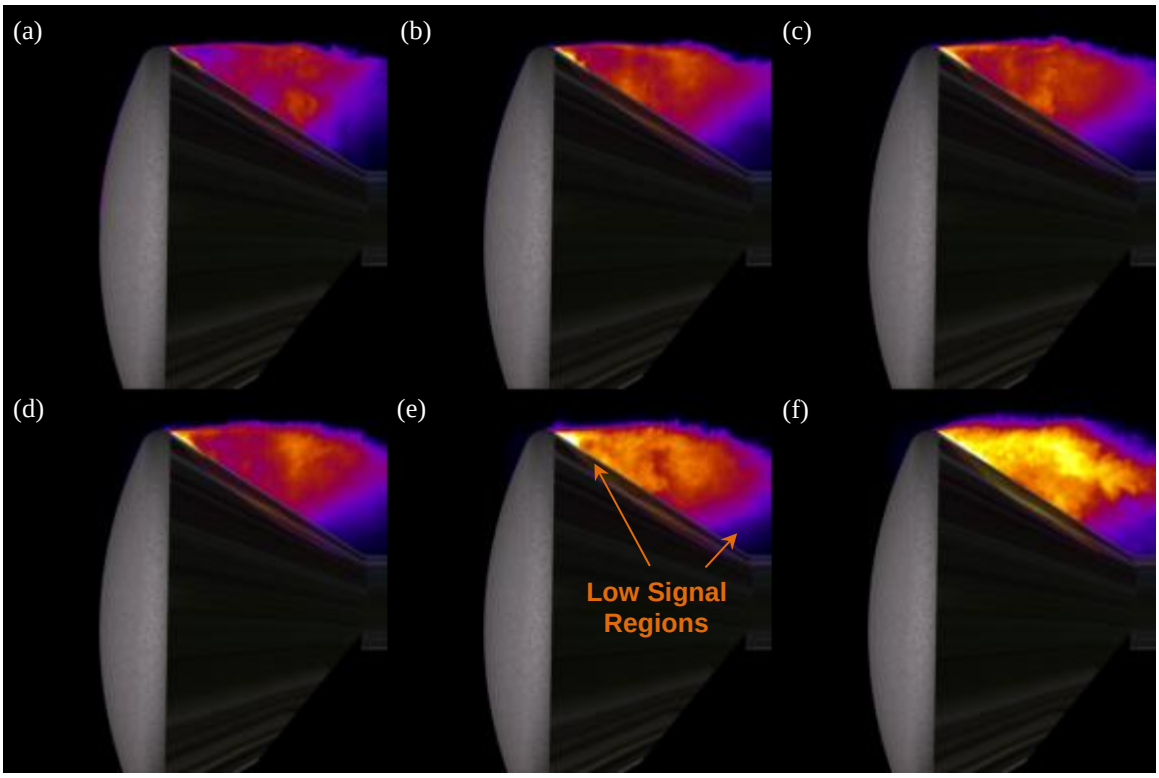

Figure 4: Naphthalene PLIF images of a capsule model at 0° angle of attack. Images were collected during one run and images a-f are sequential in time, separated by approximately ten seconds.

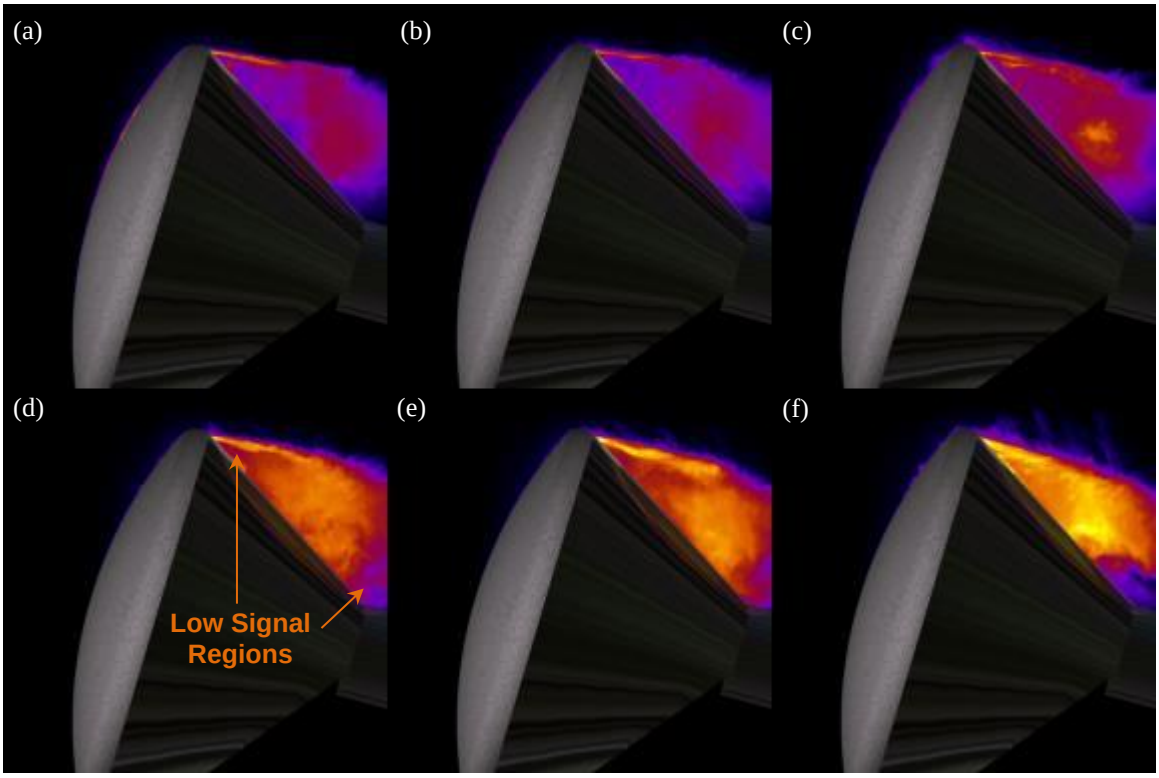

Figure 5: Naphthalene PLIF images of a capsule model at 12° angle of attack. Images were collected during one run and images a-f are sequential in time, separated by approximately ten seconds.

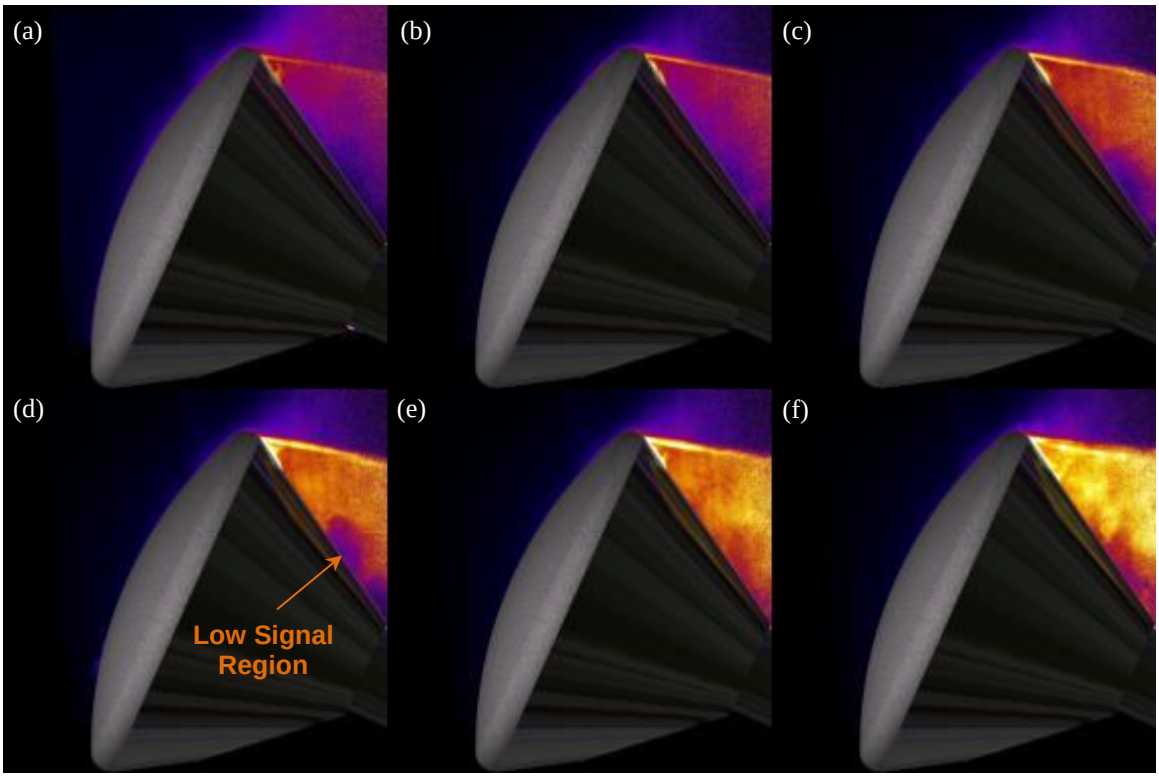

Figure 6: Naphthalene PLIF images of a capsule model at 24° angle of attack. Images were collected during one run and images a-f are sequential in time, separated by approximately ten seconds.

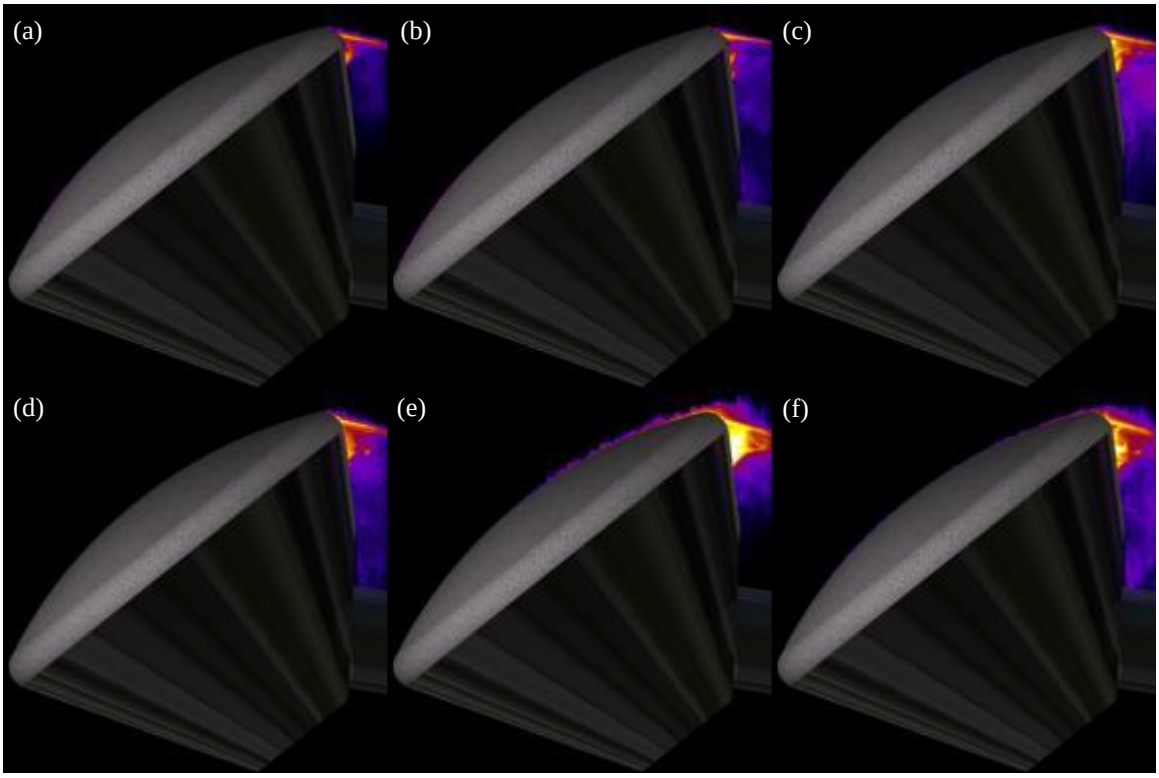

Figure 7: Naphthalene PLIF images of a capsule model at 52° angle of attack. Images were collected during one run and images a-f are sequential in time, separated by approximately ten seconds.

Figures 8 through 11 depict the capsule model at various angles of attack with instantaneous naphthalene PLIF images superimposed on instantaneous Schlieren images. The naphthalene PLIF and Schlieren images were not collected simultaneously. An aluminum heat shield was used for the Schlieren imaging so the Schlieren shows no effects of ablation. In these figures a bow shock can be seen in front of the model and expansion fans are visible off both shoulders. Less obvious—and seen most clearly in Figure 8a—are the shear layer and lip shock just downstream of the capsule shoulders. Shocks occurring as a result of the presence of the sting are seen in Figures 9 through 11. Also, a third expansion fan is visualized in Figure 11 emanating from the aft edge of the windward capsule afterbody. These visualizations provide a way to view the naphthalene PLIF images in the context of the main features of the flowfield. One comparison that can be made between the Schlieren images and the naphthalene PLIF images is the location of the shear layer, which compares favorably in the figures below. The PLIF images show detailed information about the state of the boundary layer and shear layer that is not seen clearly in the Schlieren images. Furthermore, since the PLIF technique makes measurements on a planar slice whereas Schlieren images are path averaged, local flow information can be identified. However, the PLIF images do not visualize the flow features away from the model (i.e. shocks and expansion fans), hence the complimentary nature of the two techniques.

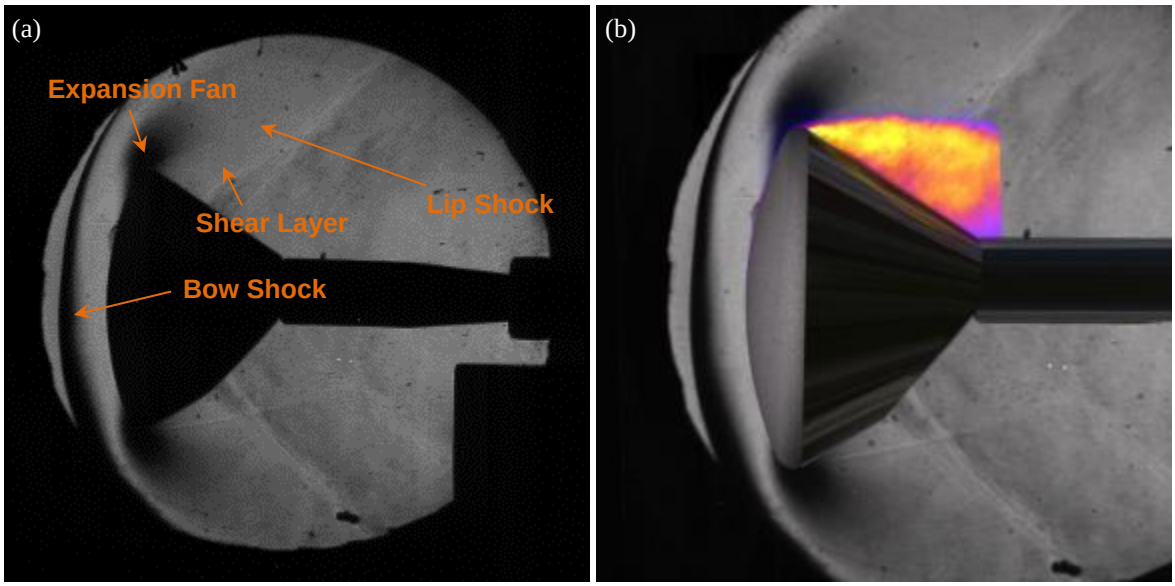

Figure 8: Orion capsule model in a Mach 5 flow at 0° angle of attack with (a) Schlieren visualization and (b) naphthalene PLIF image superimposed on a Schlieren visualization of the flowfield.

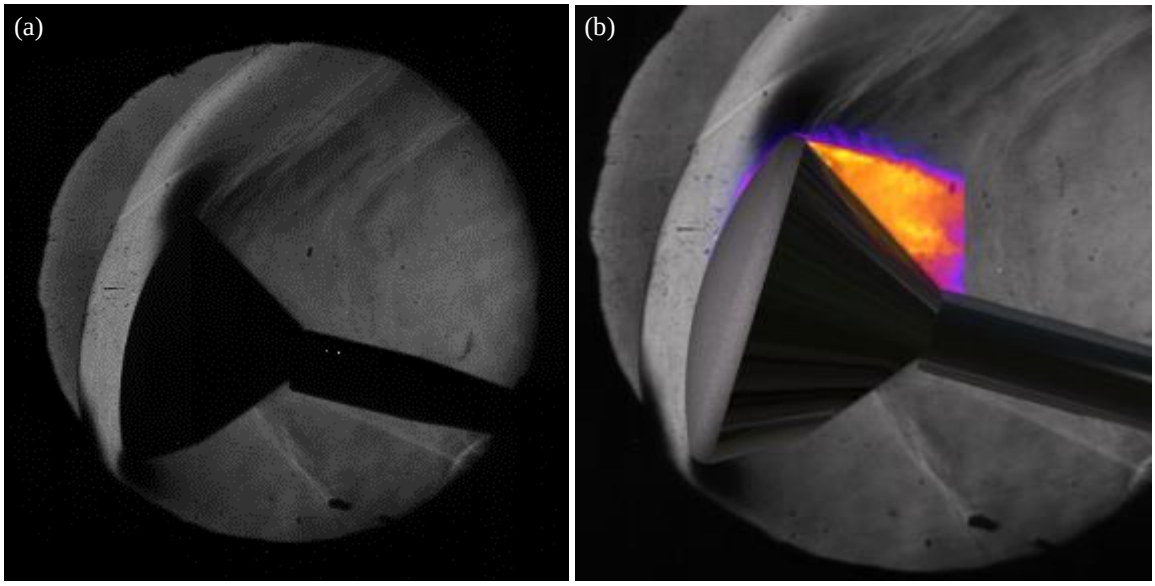

Figure 9: Orion capsule model in a Mach 5 flow at 12° angle of attack with (a) Schlieren visualization and (b) naphthalene PLIF image superimposed on a Schlieren visualization of the flowfield.

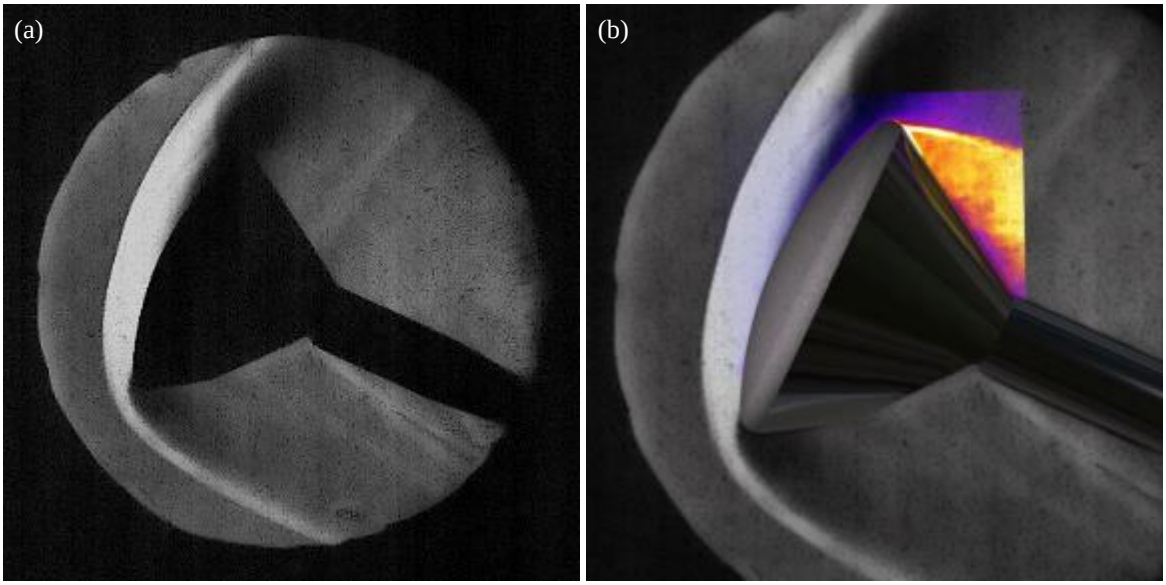

Figure 10: Orion capsule model in a Mach 5 flow at 24° angle of attack with (a) Schlieren visualization and (b) naphthalene PLIF image superimposed on a Schlieren visualization of the flowfield.

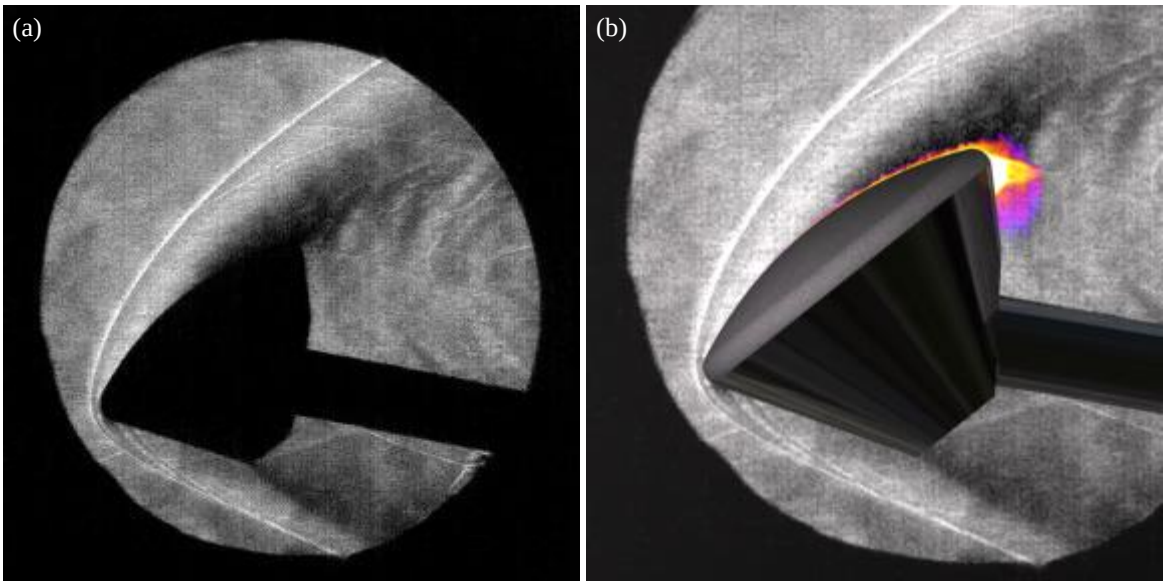

Figure 11: Orion capsule model in a Mach 5 flow at 52° angle of attack with (a) Schlieren visualization and (b) naphthalene PLIF image superimposed on a Schlieren visualization of the flowfield.

IV. Conclusion

Naphthalene PLIF has been used to visualize the dispersion of gas-phase ablation products on a scaled Orion MPCV model at four different angles of attack in the Mach 5 wind tunnel facility at The University of Texas at Austin. With this set of experiments, it was demonstrated that naphthalene PLIF was a viable technique for imaging ablation products transport on a reentry capsule geometry. The naphthalene PLIF flow visualization was complemented by Schlieren imaging, and the structure of the capsule shear layer compared favorably when imaged with both techniques. In the naphthalene PLIF images, high concentrations of scalar were imaged in the capsule wake region. Additionally, intermittent turbulent structures were visualized on the heat shield surface, particularly for the 12° and 52° AoA cases. The most prominent structures seen on the heat shield occurred for the 52° case, which consistently led to the visualization of turbulent naphthalene structures on the heat shield surface. The shear layer appeared to be laminar in the 24° case, whereas in the 12° and 0° cases the shear layer appeared to transition from laminar to turbulent (or at least became more unsteady) over the course of the run. Due to the positioning of the laser sheet, not enough naphthalene vapor was visualized in the shear layer for the 52° case to make a determination as to the nature of the shear layer. In general, the shear layer appeared to be more unsteady at lower angles of attack. Additionally, the shear layer became increasingly unsteady over the course of a wind tunnel run, most likely due to increased surface deformation and roughness, and possibly the increased blowing rate. The PLIF images also demonstrated that the model would heat up over the course of a wind tunnel run, leading to more ablation and significantly more naphthalene present in the afterbody separated flow region. Several other interesting flow features were identified in the PLIF images as well. First, the shear layer appeared to be more steady at the leeward capsule shoulder compared to further downstream, which was consistent with previous research. Also, regions of relatively low naphthalene signal were identified in the capsule wake region. These low signal regions are most likely the result of spanwise structures, such as vortices, on the capsule afterbody. A series of elongated naphthalene structures emanating from the upper edge of the shear layer were identified in multiple images as well, but the cause of this flow feature is currently undetermined.

Acknowledgements

This work was supported by a NASA Office of the Chief Technologist's Space Technology Research Fellowship Grant (#NNX11AN55H).

References

[1] Smits, A. J., Martin, M. P., and Girimaji, S., "Current status of basic research in hypersonic turbulence," AIAA 2009-151, 47th AIAA Aerospace Sciences Meeting and Exhibit, Orlando, Florida, 2009.

[2] Ho, D. W. K., Koo, J. H., Bruns, M. C., and Ezekoye, O. A., "A Review of Numerical and Experimental Characterization of Thermal Protection Materials – Part III. Experimental Testing," AIAA 2007-5773, 43rd AIAA/ASME/SAE/ASEE Joint Propulsion Conference & Exhibit, Cincinnati, Ohio, 2007.

[3] Lochman, B. 2010. Technique for Imaging Ablation-Products Transported in High-Speed Boundary Layers by using Naphthalene Planar Laser-Induced Fluorescence. Master's Thesis, University of Texas at Austin.

[4] Charwat, A. F., "Exploratory studies on the sublimation of slender camphor and naphthalene models in a supersonic wind-tunnel," 1968.

[5] Lipfert, F. and Genovese, J., "An experimental study of the boundary layers on low-temperature subliming ablators," AIAA Journal, Vol. 9, No. 7, 1971, pp. 1330-1337.

[6] Stock, H. W. and Ginoux, J. J., "Experimental Results on Crosshatched Ablation Patterns," AIAA Journal, Vol. 9 No. 5, 1971, pp. 971-973.

[7] Callaway, D. W., Reeder, M. F., Greendyke, R. B., and Gosse, R., "Photogrammetric Measurement of Recession Rates of Low Temperature Ablators in Supersonic Flow," AIAA Paper 2010-1216, 48th AIAA Aerospace Sciences Meeting, Orlando, Florida, 2010.

[8] Silton, S. I. and Goldstein, D. B., "Ablation Onset in Unsteady Hypersonic Flow About Nose Tip with Cavity," Journal of Thermophysics and Heat Transfer, Vol. 14, No. 3, 2000, pp. 421-434.

[9] Kohlman, D. L. and Richardson, R. W., "Experiments on the use of dry ice ablating wind-tunnel models," Journal of Spacecraft and Rockets, Vol. 6, No. 9, 1969, pp. 1061-1063.

[10] Goldstein, R. J. and Cho, H. H., "A review of mass transfer measurements using naphthalene sublimation," Experimental Thermal and Fluid Science, Vol. 10, 1995, pp. 416-434.

[11] Schuele, C. Y. 2011. Control of Stationary Cross-Flow Modes in a Mach 3.5 Boundary Layer Using Patterned Passive and Active Roughness. Doctoral Thesis, University of Notre Dame.

[12] Obara, C. J., "Sublimating Chemical Technique for Boundary-Layer Flow Visualization in Flight Testing," Journal of Aircraft, Vol. 25, No. 6, 1988, pp. 493-498.

[13] Hanson, R. K., Seitzman, J. M., and Paul, P. H., "Planar Laser-Fluorescence Imaging of Combustion Gases," Applied Physics B, Vol. 50, 1990, pp. 441-454.

[14] Lozano, A., Yip, B., and Hanson, R. K., "Acetone: a tracer for concentration measurements in gaseous flows by planar laser-induced fluorescence," Experiments in Fluids, Vol. 13, 1992, pp. 369-376.

[15] Danehy, P. M., J. A. Wilkes, D. W. Alderfer, S. B. Jones, A. W. Robbins, D. P. Patry and R. J. Schwartz, "Planar laser-induced fluorescence (PLIF) investigation of hypersonic flowfields in a Mach 10 wind tunnel" AIAA Paper 2006-3442, AIAA AMT-GT Technology Conference, San Francisco, Jun., 2006.

[16] Gamba, M., Mungal, M. G., Hanson, R. K., "OH PLIF Imaging of the Reaction Zone in Combusting Transverse Jets in Supersonic Crossflow," 16th Int'l Symp. on Applications of Laser Techniques to Fluid Mechanics, Lisbon, Portugal, Jul. 9-12, 2012.

[17] Danehy, P. M., J. A. Inman, G. J. Brauckmann, D. W. Alderfer, S. B. Jones, and D. P. Patry, "Visualization of a Capsule Entry Vehicle Reaction-Control System (RCS) Thruster," Journal of Spacecraft and Rockets, Vol. 46, No. 1, Jan.–Feb. 2009, pp. 93–102.

[18] Alderfer, D. W., P. M. Danehy, J. A. Wilkes Inman, K. T. Berger, G. M. Buck, and R. J. Schwartz, "Fluorescence Visualization of Hypersonic Flow Over Rapid Prototype Wind-Tunnel Models" AIAA Paper 2007-1063, 45th AIAA Aerospace Sciences Meeting and Exhibit, Reno, Nevada, Jan. 8-11, 2007.

[19] Danehy, P. M., D. W. Alderfer, J. A. Inman, K. T. Berger, G. M. Buck, and R. J. Schwartz, "Fluorescence Imaging and Streamline Visualization of Hypersonic Flow Over Rapid Prototype Wind-Tunnel Models" Proc. IMechE, Part G: J. Aerospace Engineering, 222 (G5), pp. 637-651, 2008.

[20] Combs, C. S., N. T. Clemens, P. M. Danehy, B. Bathel, R. Parker, T. Wadhams, M. Holden, and B. Kirk, "NO PLIF Visualizations of the Orion Capsule in LENS-I" AIAA Paper 2013-0033 51st AIAA Aerospace Sciences Meeting and Exhibit, Grapevine, Texas, Jan. 7-10, 2013.

[21] Kaiser, S. A. and M. B. Long, "Quantitative planar laser-induced fluorescence of naphthalene as fuel tracers," Proceedings of the Combustion Institute, Vol. 30, 2005, pp. 1555-1563.

[22] Inman, J. A., P. M. Danehy, D. W. Alderfer, and G. M. Buck, A. McCrea, and R. J. Schwartz, "PLIF Imaging of Capsule RCS Jets and Simulated Forebody Ablation" AIAA Paper 2008-0248, 46th AIAA Aerospace Sciences Meeting and Exhibit, Reno, Nevada, Jan. 7-10, 2008.

[23] Kruif, C. G. de, T. Kuipers, J.C. van Miltenburg, R.C.F. Schaake, and G. Stevens, "The vapour pressure of solid and liquid naphthalene," Journal of Chemical Thermodynamics, Vol. 13, No. 11, 1981, pp. 1081-1086.

[24] Du, H., R. A. Fuh, J. Li, Corkan, A., and Lindsey, J. S., "PhotochemCAD: A computer-aided design and research tool in photochemistry," Photochemistry and Photobiology, Vol. 68, 1998, pp. 141-142.

[25] R. J. Schwartz, "ViDI: Virtual Diagnostics Interface Volume 1-The Future of Wind Tunnel Testing" Contractor Report NASA/CR-2003-212667, Dec. 2003.

[26] Autodesk 3ds Max Product Information, Autodesk Inc., http://usa.autodesk.com/adsk/servlet/index?id=5659302&siteID=123112, viewed Jan 2, 2006.

[27] D. W. Alderfer, P. M. Danehy, J. A. Wilkes Inman, K. T. Berger, G. M. Buck, and R. J. Schwartz, "Fluorescence Visualization of Hypersonic Flow Over Rapid Prototype Wind-Tunnel Models" AIAA Paper 2007-1063, 45th AIAA Aerospace Sciences Meeting and Exhibit, Reno, Nevada, Jan. 8-11, 2007.